BJP British Journal of Pharmacology

DOI:10.1111/bph.12821
www.brjpharmacol.org

RESEARCH PAPER

(4-[6-(4-isopropoxyphenyl) pyrazolo [1,5-a]pyrimidin-3-yl] quinoline) is a novel inhibitor of autophagy

Yue Sheng, Bo Sun, Wen-Ting Guo, Xiao Liu, Yu-Chun Wang, Xin Xie, Xiao-Lin Xiao, Na Li and De-Li Dong

Department of Pharmacology (the State-Province Key Laboratories of Biomedicine-Pharmaceutics of China, Key Laboratory of Cardiovascular Research, Ministry of Education), Harbin Medical University, Harbin, Heilongjiang, China

Correspondence
Professor De-Li Dong, Department of Pharmacology, Harbin Medical University, Baojian Road 157, Harbin, Heilongjiang Province 150086, China. E-mail: dongdeli@ems.hrbmu.edu.cn

Received
7 January 2014
Revised
6 June 2014
Accepted
9 June 2014

BACKGROUND AND PURPOSE

Autophagy is an important intracellular degradation system, which is related to various diseases. In preliminary experiments we found that D4-[6-(4-isopropoxyphenyl)pyrazolo [1,5-a]pyrimidin-3-yl] quinoline (DMH1) inhibited autophagy responses. However DMH1 also inhibits the signalling pathway activated by bone morphogenetic protein-4 (BMP4). The aim of the present study was to elucidate the inhibitory effects of DMH1 on autophagy and the underlying mechanisms.

EXPERIMENTAL APPROACH

The effects of DMH1 on autophagy responses were evaluated in cultures of different cell types and with different stimuli to induce autophagy, using Western blots, transmission electron microscopy and fluorescent microscopy.

KEY RESULTS

DMH1 inhibited starvation-induced autophagy in cardiomyocytes, HeLa and MCF-7 cells, without involving the signalling pathway of BMP4. DMH1 inhibited aminoimidazole carboxamide ribonucleotide (AICAR)- and rapamycin-induced autophagy in HeLa and MCF-7 cells. DMH1 reversed starvation- and AICAR-induced inhibition of Akt, mammalian target of rapamycin (mTOR) and p70S6 kinase (S6K), and reversed rapamycin-induced inhibition of mTOR and S6K. DMH1 reversed starvation-induced decrease of the phosphorylated form of glycogen synthase kinase-3 in MCF-7 and HT29 cells. Activation of Akt and inhibition of autophagy induced by DMH1 were antagonized by an Akt specific inhibitor or by small interfering RNA for Akt in HeLa cells.

CONCLUSION AND IMPLICATIONS

DMH1 inhibited cellular autophagy responses in a range of cell types and the underlying mechanisms include activation of the Akt pathway.

Abbreviations

AICAR, aminoimidazole carboxamide ribonucleotide; BMP4, bone morphogenetic protein-4; DMH1, 4-[6-(4-isopropoxyphenyl)pyrazolo [1,5-a]pyrimidin-3-yl] quinoline; GSK3, glycogen synthase kinase 3; mTOR, mammalian target of rapamycin; S6K, p70S6 kinase; TEM, transmission electron microscopy

© 2014 The British Pharmacological Society

Table of Links

TARGETS	LIGANDS
Akt (protein kinase B)	BMP4
glycogen synthase kinase (GSK)-3	Chloroquine
mTOR	Rapamycin

This Table lists key protein targets and ligands in this article which are hyperlinked to corresponding entries in http://www.guidetopharmacology.org, the common portal for data from the IUPHAR/BPS Guide to PHARMACOLOGY (Pawson *et al.*, 2014) and are permanently archived in the Concise Guide to PHARMACOLOGY 2013/14 (Alexander *et al.*, 2013a, Alexander *et al.*, 2013b).

Introduction

Autophagy is an intracellular bulk degradation process involving sequestration of cell structures in double-membrane organelles and their delivery to lysosomes for degradation. Under normal conditions, the function of autophagy is to remove malfunctioning organelles or damaged proteins and to maintain cellular homeostasis, but when this process is extensive, autophagy acts as a cell death pathway (Yang and Klionsky, 2010).

The low MW compound, 4-[6-(4-isopropoxyphenyl) pyrazolo [1,5-a]pyrimidin-3-yl] quinoline (DMH1) (chemical structure is shown in Supporting Information Fig. S1A) is a highly selective inhibitor of the signalling pathway initiated by bone morphogenetic protein (BMP) (Hao *et al.*, 2010) and pathological cardiac hypertrophy mediated by BMP4 was inhibited by DMH1 (Sun *et al.*, 2013). Because pressure-overload induced cardiac autophagy and suppression of autophagy attenuated cardiac hypertrophy (Zhu *et al.*, 2007; Cao *et al.*, 2011; Sun *et al.*, 2013), we hypothesized that the autophagy process might be involved in DMH1-induced inhibition of cardiac hypertrophy. However, we found, surprisingly, that DMH1 inhibited starvation-induced autophagy in cardiomyocytes, HeLa and MCF-7 cells, but BMP4 and the BMP4 inhibitor noggin were without effect, indicating that DMH1 inhibited autophagy independently of the BMP4 pathway. So the aim of the present work was to elucidate the inhibitory effects of DMH1 on autophagy and the underlying mechanisms.

Methods

Cell culture

Primary cultures of cardiomyocytes were prepared from the ventricles of 1-day-old neonatal Wistar rats as previously described (Dong *et al.*, 2010; Sun *et al.*, 2013). Cardiomyocytes, MCF-7 (human breast cancer) cells (Type Culture Collection of the Chinese Academy of Sciences, Shanghai, China) and HeLa (human cervical carcinoma) and HT29 (human colon adenocarcinoma) cells (Type Culture Collection of the Chinese Academy of Sciences) were maintained in DMEM/high glucose supplemented with 10% FBS, 100 units·mL^{-1} penicillin and 100 μg·mL^{-1} streptomycin at 37°C, 5% CO_2. Cells were rested for 24 h and then treated with starvation, the mTOR inhibitor rapamycin, the AMPK activator, aminoimidazole carboxamide ribonucleotide (AICAR), and/or DMH1 or the lysosomal inhibitor chloroquine. For starvation, cells were washed with PBS and incubated in serum-free DMEM with low glucose. The time of treatment and the concentration of agents were shown in the Figures and/or corresponding Figure legends. Unless otherwise stated, the starvation condition was serum-free DMEM (5.5 mM glucose).

Transmission electron microscopy (TEM)

TEM was performed to identify autophagy and intracellular autophagolysosomes. The cells were fixed with ice-cold 2.5% glutaraldehyde in PBS (pH 7.3) at 4°C for 4 h. Fixed cells were post-fixed in 2% OsO_4, dehydrated in graded alcohol, embedded in Epon 812 (Electron Microscopy Sciences, Fort Washington, PA, USA), sectioned with an ultramicrotome, and stained with uranyl acetate and lead citrate. The sections were examined with a TEM (Technai 10, Philips, The Netherlands).

Western blot analysis

Cells were lysed with RIPA buffer containing 1% protease inhibitor and centrifuged at 13 500× *g* for 15 min at 4°C. The supernatants were collected, and the protein concentrations were determined with BCA Protein Assay Kit (Bio-Rad, Hercules, CA, USA). The proteins were separated by electrophoresis in 8–15% SDS-PAGE gels and transferred to nitrocellulose membranes. After blocking with 5% non-fat dry milk in PBS for 2 h at room temperature, the membranes were incubated with the primary antibodies against LC3B (1:2000), AMPK (1:200), phospho-AMPK (Thr^{172}) (1:500), mTOR (1:500), phospho-mTOR (Ser^{2448}) (1:500), Akt (1:1000), phospho-Akt (Ser^{473}) (1:1000), p70S6K (1:500), phospho-p70S6K (Thr^{389}) (1:500), SQSTM1/p62 (1:1000), actin (1:1000) at 4°C overnight. After washing with PBS-0.1% Tween 20 (PBST), membranes were incubated with fluorescence-conjugated goat anti-rabbit IgG or goat anti-mouse IgG secondary antibody (Invitrogen, Carlsbad, CA, USA 1:10 000) at room temperature for 1 h. The band densities were quantified by densitometry using Odyssey v3.0 software (LI-COR Inc., Lincoln, NE, USA).

Autophagy detection by GFP-LC3

GFP-LC3 expression constructs were a kind gift from Dr Honglin Luo (The iCAPTURE Center, St. Paul's Hospital/Providence Health Care – University of British Columbia, Vancouver, British Columbia, Canada). The cells were seeded onto coverslips placed onto a six-well plate. After overnight culture, cells were transfected with 3 μg GFP-LC3 expressing

plasmid using a mixture of Lipofectamine 2000 reagent (Invitrogen) and GFP-LC3 plasmid in Opti-MEM medium (Life Technologies, Rockville, MD, USA) for 6 h of incubation. The medium was removed and regular complete medium was added to the wells overnight. Cells were treated with starvation in the presence or absence of DMH1 for 24 h. At the end of treatment, cells were washed twice with PBS and fixed in 4% paraformaldehyde-PBS solution for 10 min at room temperature. After washing with PBS, coverslips were mounted on a microscope slide. GFP-LC3 dots in cells were investigated by an Olympus fluorescent microscope (Olympus, Tokyo, Japan) at 400× magnification.

Data analysis

Data are presented as mean ± SEM. Student's *t*-test was used for the evaluation of statistical significance. For multiple comparisons, one-way ANOVA and Tukey's post-test was used. $P < 0.05$ was considered significant.

Materials

Rapamycin, AICAR, DMH1, chloroquine were purchased from Sigma-Aldrich (St. Louis, MO, USA). Recombinant human BMP4 and noggin were purchased from R&D Systems (Minneapolis, MN, USA). The cell culture media were Hyclone products (Logan, UT, USA). Antibody against LC3B was from Sigma-Aldrich. Antibodies against AMP-activated PK (AMPK), phospho-AMPK (Thr^{172}), mammalian target of rapamycin (mTOR), phospho-mTOR (Ser^{2448}), Akt, phospho-Akt (Ser^{473}), p70S6 kinase (70S6K), phospho-p70S6K (Thr^{389}), SQSTM1/p62, actin, glycogen synthase kinase (GSK)-3α/β and phospho-GSK-3α/β ($Ser^{21/9}$) were purchased from Cell Signaling Technology (Beverly, MA, USA). The Akt1/2 kinase inhibitor, 1,3-dihydro-1-(1-((4-(6-phenyl-1H-imidazo[4,5-g]quinoxalin-7-yl)phenyl)methyl)-4-piperidinyl)-2H-benzimidazol-2-one trifluoroacetate salt hydrate was purchased from Sigma-Aldrich. siRNA for Akt and control siRNA were purchased from Cell Signaling Technology. DMH1 was dissolved in DMSO and diluted in the culture media (0.7μL in 1000 μL). Under these conditions, these vehicles showed no effect on autophagy or cell viability (data not shown).

Results

DMH1 inhibits starvation-induced autophagy in cardiomyocytes, HeLa and MCF-7 cells

Serum depletion starvation for 24 h increased the formation of LC3-II in cardiomyocytes and this increase was inhibited by DMH1 (10 μM) treatment (Figure 1A), suggesting that DMH1 inhibited activation of autophagy. DMH1 had no effect on the basal LC3-II level (Figure 1A). Next, we starved cardiomyocytes by serum deprivation for 48 h to induce autophagy and observed the effects of BMP4, noggin and DMH1. Because BMP4 and noggin are proteins, we removed serum to avoid the interference of serum on the action of BMP4 and noggin. BMP4 (50 $ng \cdot mL^{-1}$) and noggin (100 $ng \cdot mL^{-1}$) treatment had no effect, but DMH1 treatment significantly reduced the increased formation of LC3-II induced by serum depletion (Figure 1B).

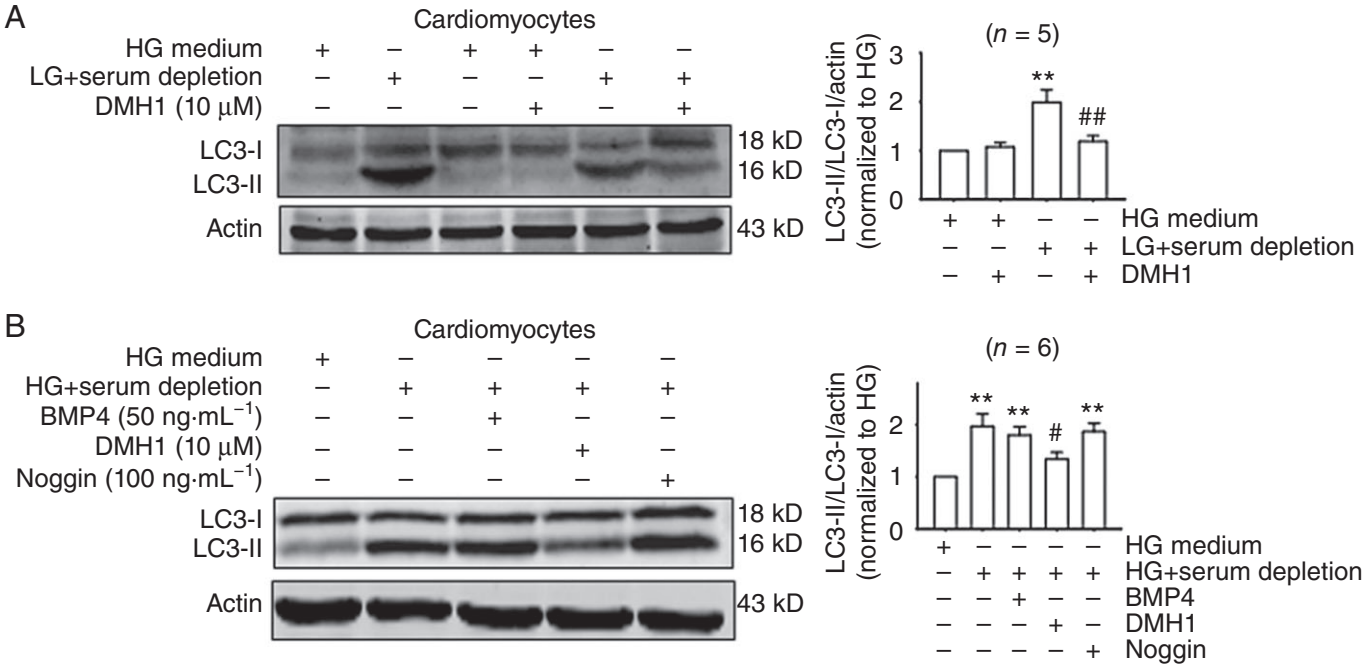

Figure 1

DMH1 inhibits starvation-induced autophagy in cardiomyocytes. (A) DMH1 inhibited autophagy in cardiomyocytes induced by serum depletion (in 5.5 mM glucose medium). Cells were cultured for 24 h.**$P < 0.01$ versus HG; ##$P < 0.01$ versus serum depletion (in 5.5 mM glucose medium). HG (25 mM) medium; low glucose (5.5 mM) medium. (B) DMH1, but neither BMP4 nor noggin inhibited autophagy induced by serum depletion in cardiomyocytes. Cells were cultured in 25 mM glucose medium for 48 h.**$P < 0.01$ versus HG; #$P < 0.05$ versus HG + serum depletion.

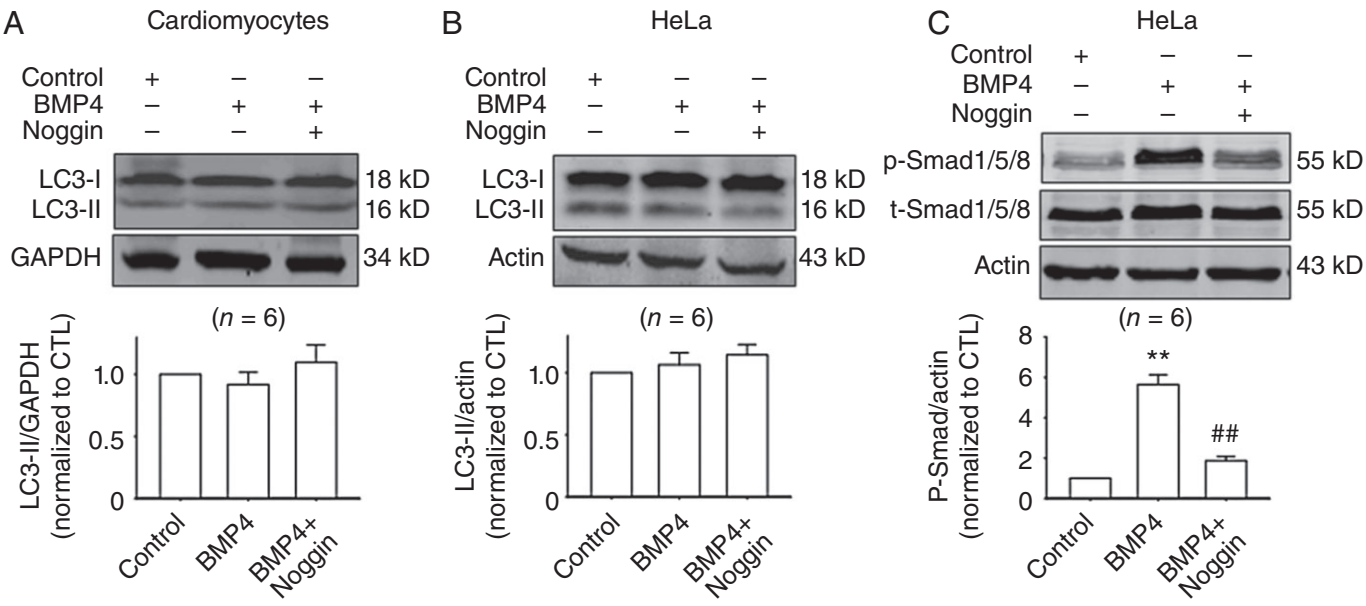

Figure 2

(A) BMP4 did not affect autophagy responses in cardiomyocytes. Cells were cultured in 25 mM glucose medium with 0.1% FBS for 48 h. The concentration of BMP4 was 50 ng·mL^{-1} and noggin was 100 ng·mL^{-1}. (B–C) BMP4 did not affect the autophagy responses in HeLa cells, but activated its downstream component, Smad. The concentration of BMP4 was 50 ng·mL^{-1} and noggin was 100 ng·mL^{-1}. Cells were cultured in 25 mM glucose medium with 0.1% FBS for 24 h. $^{**}P < 0.01$ versus control; $^{\#\#}P < 0.01$ versus BMP4. CTL, control.

Under conditions of serum depletion, the process of autophagy is already activated (Figure 1B) and thus any activation by BMP4 would be less easily observed. We therefore examined the effects of BMP4 on un-activated autophagy, under normal, basal conditions. BMP4 (50 ng·mL^{-1}) and BMP4 plus noggin (100 ng·mL^{-1}) treatments had no effect on the basal autophagy in cardiomyocytes and HeLa cells (Figure 2A, B). In order to confirm that the BMP4 pathway could be activated, we examined the effects of BMP4 on Smad1/5/8, a known downstream component of the BMP4 signalling pathway, in HeLa cells. BMP4 treatment significantly increased p-Smad1/5/8 levels and this increase was inhibited by the BMP4 inhibitor noggin (100 ng·mL^{-1}) (Figure 2C).

These data indicated that BMP4 was able to activate downstream targets in its signalling pathway, but did not affect the autophagy responses. However, DMH1 inhibited autophagy, without involving the BMP4 signalling pathway.

Then we starved HeLa cells and MCF-7 cells for further analysis of the effects of DMH1 on autophagy. Starvation accelerated autophagic flux in HeLa cells, as quantified by the difference of LC3-II in the absence and presence of the lysosomal inhibitor chloroquine (Figure 3A, panels a and b). DMH1 treatment had no effect on the basal level of LC3-II, but significantly inhibited the increased formation of LC3-II induced by starvation in HeLa cells (Figure 3B). Noggin treatment did not affect starvation-induced increase of LC3-II in HeLa cells (Figure 3B). These results were reproduced in MCF-7 cells (Figure 3C).

The inhibition of autophagy by DMH1 was further confirmed in HeLa cells using the GFP-LC3 fusion protein, an autophagy reporter widely used to visualize autophagic vacuole formation after induction of autophagy, by measuring p62 and by assessment of autophagosome formation with TEM. Results from fluorescence microscopy showed that DMH1 treatment inhibited the punctate pattern of GFP-LC3, caused by starvation stimuli (Figure 3D). p62 is a marker of autophagic flux because it accumulates when autophagy is inhibited, and it decreases when autophagy is induced. DMH1 inhibited the starvation-induced decrease of p62 accumulation (Figure 3E). TEM examination showed that a large number of cytoplasmic autophagosomes appeared after starvation treatment, but fewer autophagosomes were observed in the cells exposed to starvation plus DMH1 treatment (Figure 3F). Concentration-effect experiments with DMH1 showed that levels of DMH1 as low as 5 μM inhibited autophagy (Figure 4A). The time-course experiments showed that increasing times of starvation (6-24h) increased levels of LC-II and that DMH1 was inhibitory at all times assayed, in MCF-7 cells (Figure 4B). We then used another cell line, HT29 cells, to examine the inhibitory effects of DMH1 on starvation-induced autophagy responses. As shown in Supporting Information Fig. S2, DMH1 inhibited starvation-induced autophagy in a concentration-dependent manner and completely inhibited the increased autophagy response at 100 μM concentrations in HT29 cells. Taken together, our data showed that DMH1 inhibited autophagy and this effect was not cell-specific.

DMH1 inhibits AICAR- and rapamycin-induced autophagy

In addition to the starvation-induced autophagy, we tested the effects of DMH1 on AICAR- and rapamycin-induced autophagy in HeLa and MCF-7 cells. As shown in Figure 5A

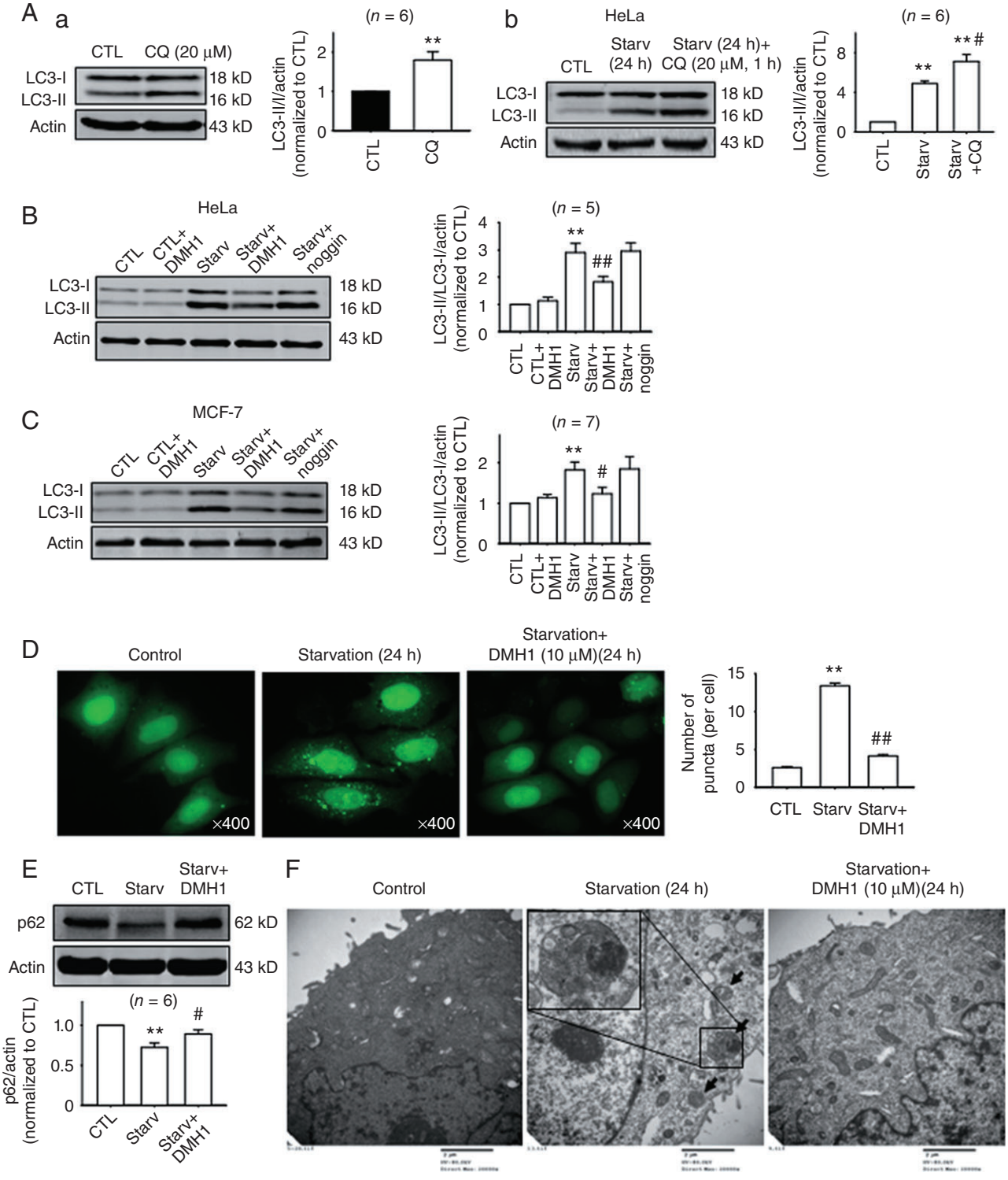

Figure 3

DMH1 inhibits starvation-induced autophagy in HeLa and MCF-7 cells. (A) Chloroquine (CQ) increased the basal LC3-II level (a) and the starvation-induced LC3-II accumulation (b) in HeLa cells. $^{**}P < 0.01$ versus control; $^{\#}P < 0.05$ versus starvation. (B and C) DMH1 (10 μM), but not noggin (100 ng·mL^{-1}) inhibited starvation-induced autophagy in HeLa and MCF-7 cells. $^{**}P < 0.01$ versus control; $^{\#}P < 0.05$, $^{\#\#}P < 0.01$ versus starvation. CTL, control; Starv, starvation. (D) DMH1 (10 μM) reduced the increased LC3-GFP punctate distribution, induced by starvation. The left was the representative image and the right was the analysed data. $^{**}P < 0.01$ versus control; $^{\#\#}P < 0.01$ versus starvation. CTL, control; Starv, starvation. (E) DMH1 (10 μM) treatment for 24 h inhibited the starvation-induced decrease of p62 accumulation $^{**}P < 0.01$ versus control; $^{\#}P < 0.05$ versus starvation. (F) Photographs from TEM showed characteristic autophagosomes (arrows) in HeLa cells after 24 h starvation. Magnification, ×20 000. CTL, control; Starv, starvation.

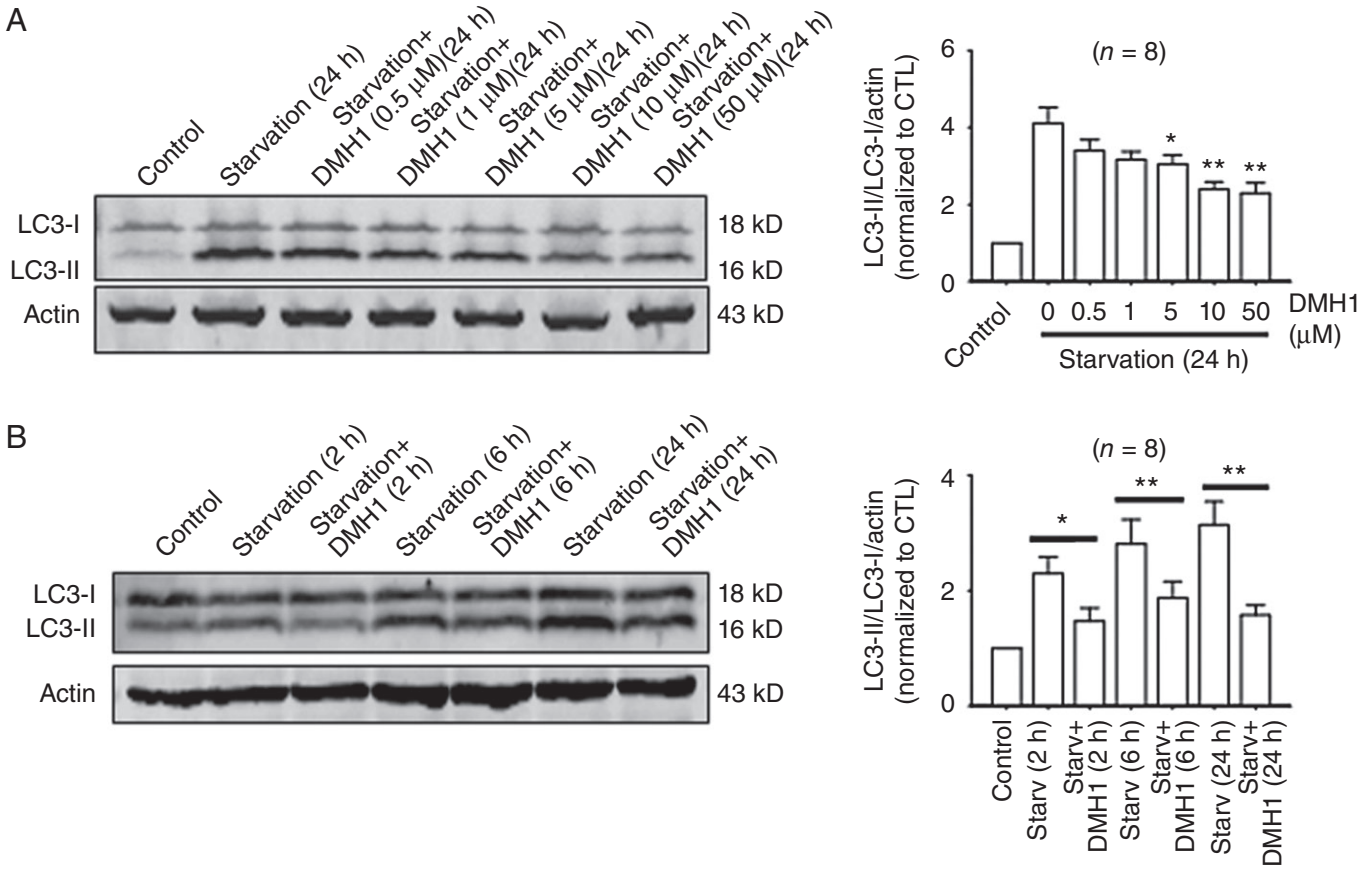

Figure 4

The concentration- and time-dependent effects of DMH1 on starvation-induced autophagy in MCF-7 cells (A) The concentration-dependent effect of DMH1 on the levels of LC3-II in MCF-7 cells. *$P < 0.05$, **$P < 0.01$ versus starvation. (B) The effect of DMH1 (10 μM) on the levels of LC3-II in MCF-7 cells subjected to different periods of starvation. *$P < 0.05$, **$P < 0.01$ versus starvation. Starv, starvation. CTL, control.

and B, DMH1 treatment inhibited the increased formation of LC3-II induced by AICAR (0.5 mM) and rapamycin (0.5 μM) in HeLa and MCF-7 cells, showing that the inhibition of autophagy by DMH1 was not model-specific.

DMH1 inhibits autophagy through Akt-dependent pathways

Activation of AMPK by starvation or AICAR induced autophagy responses (Wang *et al.*, 2009; Kim *et al.*, 2011). Given that DMH1 inhibited starvation- and AICAR-induced autophagy, we tested the effects of DMH1 on AMPK activation. As shown in Supporting Information Fig. S3, starvation and AICAR treatment significantly activated AMPK; however, DMH1 treatment showed no inhibitory effects on the AMPK activation in HeLa cells, indicating that the inhibition of autophagy by DMH1 was exerted either downstream of AMPK or by pathways other than those involving AMPK.

The Akt/mTOR/p70S6K pathway is the main regulatory pathway that suppresses autophagy (Blommaart *et al.*, 1995; Shigemitsu *et al.*, 1999; Arico *et al.*, 2001). Firstly, we examined the effects of DMH1 on the Akt/mTOR/p70S6K pathway in HeLa cells under starvation conditions. As shown in Figure 6A, starvation treatment significantly down-regulated phosphorylated Akt, mTOR and p70S6K, but these down-regulations were reversed by DMH1 treatment. AICAR not only activates AMPK, but also reduces Akt activation (King *et al.*, 2006). We therefore examined the effects of DMH1 on the Akt/mTOR/p70S6K pathway in AICAR-induced autophagy using HeLa cells. AICAR treatment down-regulated phosphorylated Akt, mTOR and p70S6K, and these down-regulations were reversed by DMH1 treatment (Figure 6B), similar to the results shown in Figure 6A.

Activated Akt leads to activation of mTOR, which results in inhibition of autophagy. As DMH1 activated Akt, we examined whether activation of mTOR was due to the activated Akt or direct activation by DMH1, using rapamycin, known to be a direct inhibitor of mTOR. Rapamycin significantly decreased phosphorylation of mTOR and p70S6K, and DMH1 treatment reversed the decreased phosphorylation of mTOR and p70S6K induced by rapamycin in HeLa cells (Figure 6C), indicating that DMH1 could also directly activate mTOR.

These data showed that DMH1 inhibited autophagy when the autophagy response was activated. We further tested the effect of DMH1 alone, in normal medium, without serum

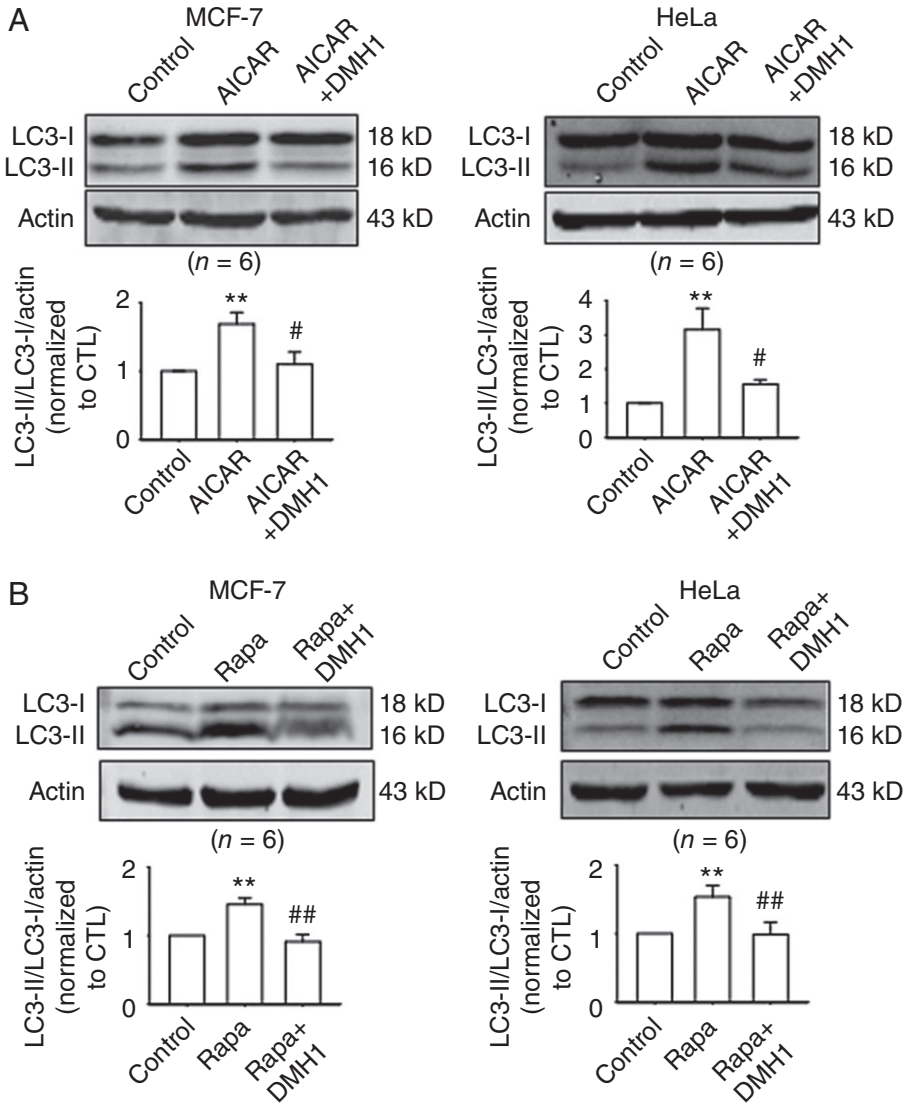

Figure 5

DMH1 inhibits AICAR- and rapamycin (Rapa)-induced autophagy in HeLa and MCF-7 cells. $^{**}P < 0.01$ versus control. $^{\#}P < 0.05$, $^{\#\#}P < 0.01$ versus respective drug treatment. The concentrations of DMH1, AICAR and rapamycin were 10 μM, 0.5 mM and 0.5 μM respectively. The treatment time was 24 h. CTL, control.

depletion. Relative to the high glucose (25 mM) medium, low glucose (5.5 mM) medium represents a starving state. Therefore, we first compared the basal level of LC3II, Akt, mTOR and S6K in the normal high glucose (HG) and low glucose (LG) medium. Results showed that, compared with HG, LG conditions showed increased LC3II expression and less activated Akt, mTOR and S6K (Figure 7A). Then, we compared the effects of DMH1 on Akt, mTOR and S6K in the normal HG and LG medium. In HG medium, DMH1 had no effects on Akt, mTOR and S6K activation (Figure 7B). However, in LG medium, DMH1 treatment increased p-Akt, p-mTOR and p-S6K levels (Figure 7C). Because the autophagy response increased and Akt, mTOR and S6K activation decreased in LG conditions, compared with HG conditions, and DMH1 activated Akt, mTOR and S6K in LG conditions, but not in HG conditions, it suggested that DMH1 activated the inhibited Akt signal and specifically inhibited the increased autophagy response.

The kinase, GSK3, is a critical downstream component of the Akt pathway and is rapidly phosphorylated at Ser^{21} in GSK-3α or Ser^{9} in GSK-3β, resulting in inhibition of GSK-3 activity. We further examined the effects of DMH1 on the starvation-induced increase of GSK3 activity. As shown in Supporting Information Fig. S4, serum starvation decreased levels of phospho-GSK-3α/β in MCF-7 and HT29 cells, and these effects were reversed by DMH1 treatment.

Our data, so far, showed that DMH1 inhibited autophagy responses and reversed the inhibition of Akt/mTOR/p70S6K, induced by different stimuli of autophagy. However, it was not clear if DMH1 inhibited autophagy through activating

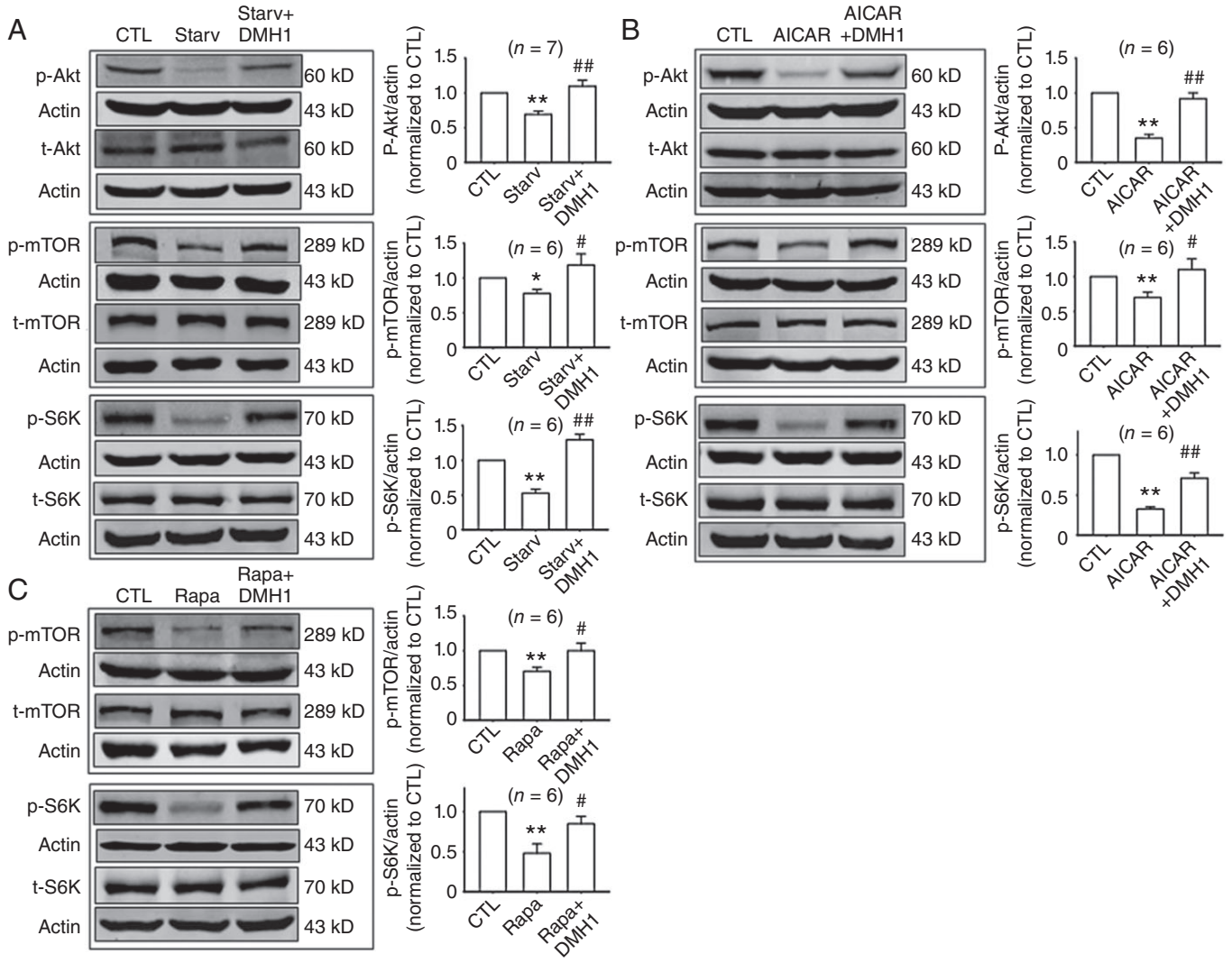

Figure 6

DMH1 activates Akt/mTOR pathway. (A) DMH1 (10 μM) treatment reversed the starvation-induced down-regulation of phosphorylated Akt, mTOR and p70S6K. *P < 0.05, **P < 0.01 versus control; #P < 0.05, ##P < 0.01 versus starvation. The incubation time was 24 h. (B) DMH1 treatment reversed the AICAR-induced down-regulation of phosphorylated Akt, mTOR and p70S6K. **P < 0.01 versus control; #P < 0.05, ##P < 0.01 versus AICAR. The concentrations of DMH1 and AICAR were 10 μM and 0.5 mM. The incubation time was 24 h. (C) DMH1 treatment reversed the rapamycin (Rapa)-induced down-regulation of phosphorylated mTOR and p70S6K. **P < 0.01 versus control; #P < 0.05 versus rapamycin. The concentrations of DMH1 and rapamycin were 10 μM and 0.5 μM. The incubation time was 24 h. CTL, control; Starv, starvation.

the Akt pathway. Therefore, we used the Akt-specific inhibitor and Akt siRNA to inhibit Akt function and expression. As shown in Figure 8A, the Akt inhibitor (0.5 μM) inhibited DMH1-induced Akt activation and DMH1-induced inhibition of autophagy, indicating that Akt activation was involved in DMH1-induced autophagy inhibition. However, it was noticeable that, when Akt function and expression were suppressed by the Akt inhibitor or Akt siRNA, as shown in Figure 8A (p-Akt in Starv + Akti group) and Figure 8B (t-Akt and p-Akt in Akt siRNA group), DMH1 still showed inhibitory effects on autophagy (Figure 8A, B), indicating that there were signal pathways, other than Akt activation, involved in DMH1-induced inhibition. Indeed, as shown in Figure 6C, DMH1 directly activated mTOR/p70S6K.

Discussion and conclusions

We have shown that DMH1 inhibited cell autophagy responses and the underlying mechanisms appeared to involve activation of the Akt pathway. In the present study, inhibition of autophagy by DMH1 was demonstrated in three different models, induced by starvation, AICAR or rapamycin and in four different cell types, cardiomyocytes, HeLa, MCF-7 and HT29 cells, indicating that the inhibition of autophagy by DMH1 was not cell- or model-specific. Therefore, we used HeLa cells to elucidate the mechanism of DMH1 action.

mTOR is a key regulator of autophagy (Jung *et al.*, 2010) and AMPK inhibits and Akt activates mTOR (Gwinn *et al.*, 2008). We found that DMH1 did not block AMPK activation,

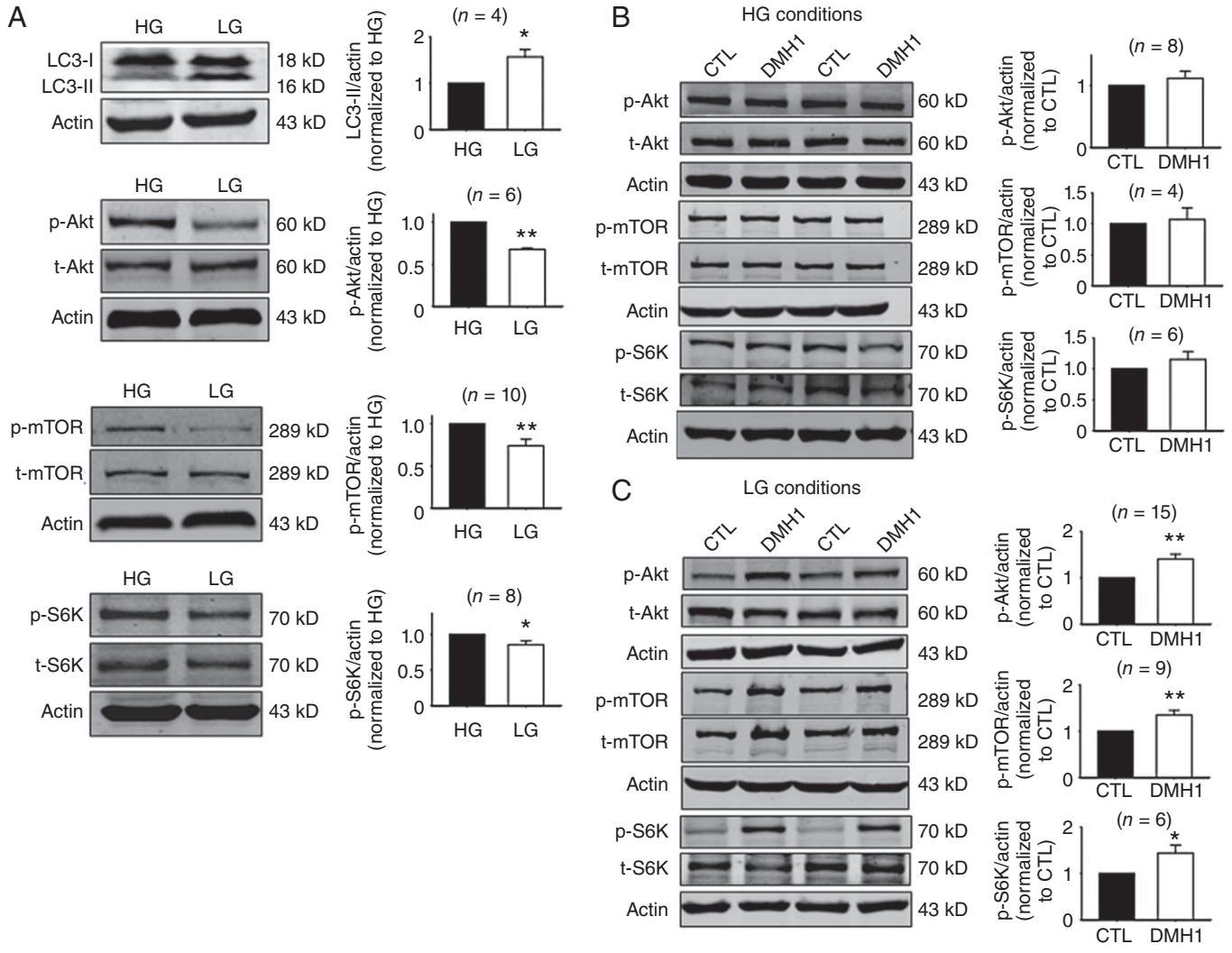

Figure 7

DMH1 inhibits the activated autophagy response. (A) The basal level of LC3II, Akt, mTOR and S6K in the normal HG and LG medium. *$P < 0.05$, **$P < 0.01$ versus HG. (B) DMH1 (10 μM) had no effects on the basal Akt, mTOR and S6K activity in the normal HG medium. (C) DMH1 (10 μM) treatment increased p-Akt, p-mTOR and p-S6K levels in the normal LG medium. *$P < 0.05$, **$P < 0.01$ versus control. CTL, control.

but activated Akt. In rapamycin-induced autophagy, DMH1 directly activated the rapamycin-inhibited mTOR (Figure 6C). Thus, the activation of mTOR by DMH1 derived from two actions, a direct activation of mTOR and, indirectly through Akt activation. These results also explained why DMH1 did not block AMPK activation itself (Supporting Information Fig. S3), but still blocked AMPK activation-induced autophagy (Figure 5A).

DMH1is a compound C analogue with structural modifications at the 3- and 6-positions in the pyrazolo[1,5-a]pyrimidine backbone (Supporting Information Fig. S1A, B) (Hao *et al.*, 2010). Compound C is a potent, selective AMPK inhibitor, but DMH1 showed no inhibitory effects on AMPK activation as shown by our present data and other studies (Hao *et al.*, 2010). However, DMH1 and compound C exerted completely opposing effects on autophagy and the Akt/mTOR pathway. From our data, DMH1 inhibited autophagy mainly through activating the Akt/mTOR pathway, whereas earlier work with compound C showed it induced autophagy through *inhibiting* the Akt/mTOR pathway in U251 human glioma, C6 rat glioma, L929 mouse fibrosarcoma and B16 mouse melanoma cells (Vucicevic *et al.*, 2011). These results indicated that the opposing effects of DMH1 and compound C on autophagy were not cell-specific. Based on the similar structure of DMH1 and compound C and their opposing effects on the Akt/mTOR pathway, we postulate that there might be a common target that binds to DMH1 and compound C, and the binding state of the target would determine the different functional consequences. DMH1 and compound C could activate and inhibit Akt/mTOR pathway, respectively, but it was still unclear whether these compounds influenced Akt activity directly or were indirect, influencing some upstream component in the Akt signalling pathway.

Autophagy can be suppressed at any stage of the autophagic process. At this time, many inhibitors have been identified, including 3-methyladenine (3-MA), wortmannin,

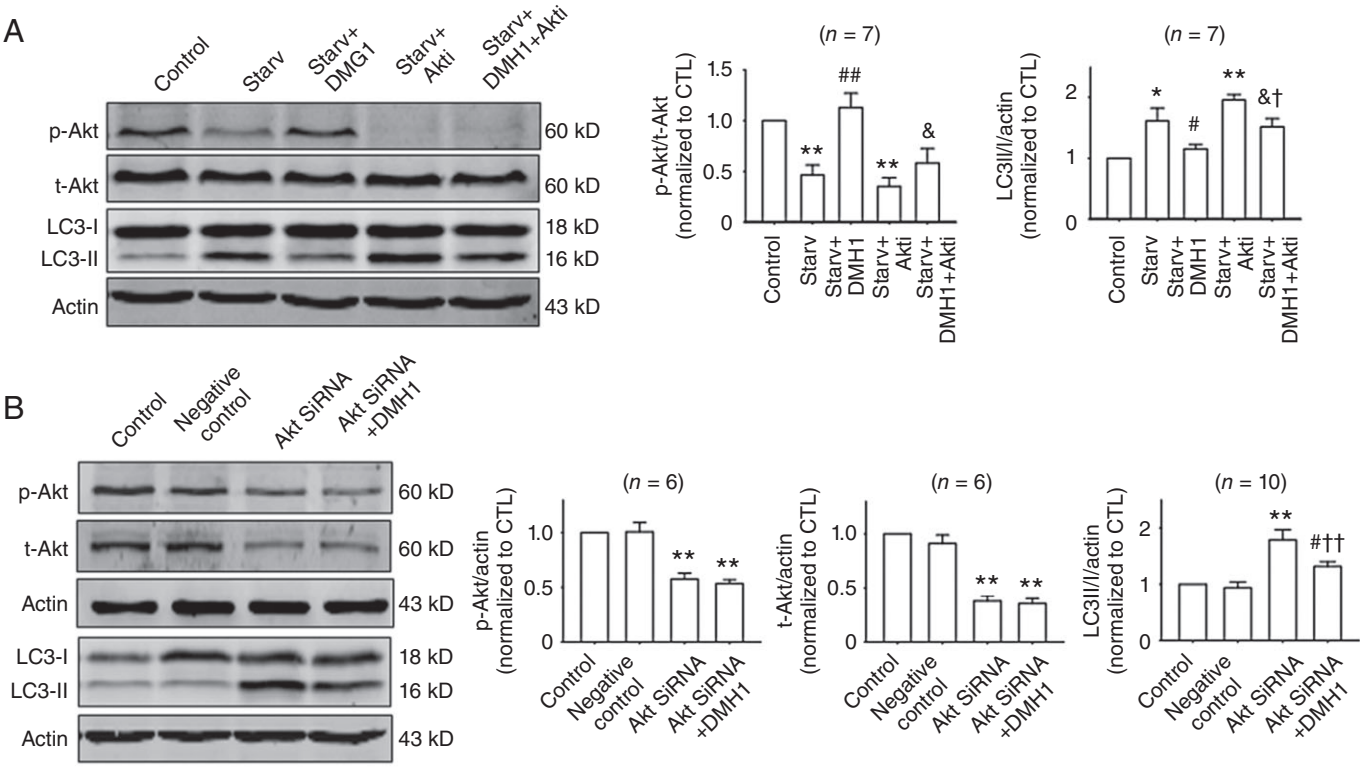

Figure 8

(A) Akt inhibitor inhibited DMH1-induced Akt activation and DMH1-induced autophagy inhibition, $^{**}P < 0.01$ versus control; $^{\#}P < 0.05$, $^{\#\#}P < 0.01$ versus Starv; $\&P < 0.05$ versus Starv + DMH1. $\dagger P < 0.05$ versus Starv + Akti. The concentrations of DMH1 and Akti were 10 and 0.5 μM. (B) Akt siRNA (50 nM) inhibited Akt expression and induced autophagy, and DMH1 (10 μM) inhibited Akt siRNA-induced autophagy. $^{**}P < 0.01$ versus control; $^{\#}P < 0.05$ versus Akt siRNA; $\dagger\dagger P < 0.01$ versus control. Because both total Akt and phosphorylated Akt decreased in Akt siRNA and Akt siRNA + DMH1 groups, the p-Akt/actin and t-Akt/actin were used for analysis. CTL, control; Starv, starvation.

LY294002, cycloheximide, bafilomycin A1 and chloroquine (Yang *et al.*, 2013). These compounds inhibit autophagy responses through different mechanisms. Thus, 3-MA, wortmannin and LY294002 suppress autophagy via inhibition of class III PI3K and cycloheximide inhibits protein biosynthesis. Bafilomycin A1 is a specific inhibitor of vacuolar-type H^+-ATPases, which are within the membranes of many organelles including lysosomes, endosomes and secretory vesicles. Chloroquine is a lysosomal lumen alkalizer and its accumulation inside the acidic parts of the cell leads to inhibition of lysosomal enzymes and blocks the fusion of endosomes and lysosomes. Some autophagy inhibitors are not specific for autophagy and have to be used at higher concentrations or doses. For example, the classical autophagy inhibitor 3-MA is generally used as high as 10 mM (Li *et al.*, 2009; Wong *et al.*, 2011). Our previous study also showed that 3-MA induced cell death, independently of autophagy inhibition (Sheng *et al.*, 2013). The present study provides a new inhibitor for further studies of autophagy.

Acknowledgements

This work was supported by the National Natural Science Foundation of China (81373406, 81173049) and the Chang Jiang Scholar Candidates Program for Provincial Universities in Heilongjiang (2011CJHB002).

Author contributions

Y. S., W.-T. G., N. L., X. L., X. X., X.-L. X., Y.-C. W. and B. S. performed the cell culture and Western blot experiments. D.-L. D. designed the project and wrote the paper.

Conflict of interest

The authors declare no conflict of interest.

References

Alexander SPH, Benson HE, Faccenda E, Pawson AJ, Sharman JL, McGrath JC *et al.* (2013a). The concise guide to PHARMACOLOGY 2013/14: overview. Br J Pharmacol 170: 1449–1458.

Alexander SPH, Benson HE, Faccenda E, Pawson AJ, Sharman JL, Spedding M *et al.* (2013b). The concise guide to PHARMACOLOGY 2013/14: G protein-coupled receptors. Br J Pharmacol 170: 1459–1581.

Arico S, Petiot A, Bauvy C, Dubbelhuis PF, Meijer AJ, Codogno P *et al*. (2001). The tumor suppressor PTEN positively regulates macroautophagy by inhibiting the phosphatidylinositol 3-kinase/protein kinase B pathway. J Biol Chem 276: 35243–35246.

Blommaart EFC, Luiken JJFP, Blommaart PJE, van Woerkom GM, Meijer AJ (1995). Phosphorylation of ribosomal protein S6 is inhibitory for autophagy in isolated rat hepatocytes. J Biol Chem 270: 2320–2326.

Cao DJ, Wang ZV, Battiprolu PK, Jiang N, Morales CR, Kong Y *et al*. (2011). Histone deacetylase (HDAC) inhibitors attenuate cardiac hypertrophy by suppressing autophagy. Proc Natl Acad Sci U S A 108: 4123–4128.

Dong DL, Chen C, Huo R, Wang N, Li Z, Tu YJ *et al*. (2010). Reciprocal repression between microRNA-133 and calcineurin regulates cardiac hypertrophy: a novel mechanism for progressive cardiac hypertrophy. Hypertension 55: 946–952.

Gwinn DM, Shackelford DB, Egan DF, Mihaylova MM, Mery A, Vasquez DS *et al*. (2008). AMPK phosphorylation of raptor mediates a metabolic checkpoint. Mol Cell 30: 214–226.

Hao J, Ho JN, Lewis JA, Karim KA, Daniels RN, Gentry PR *et al*. (2010). *In vivo* structure – activity relationship study of dorsomorphin analogues identifies selective VEGF and BMP inhibitors. ACS Chem Biol 5: 245–253.

Jung CH, Ro S-H, Cao J, Otto NM, Kim D-H (2010). mTOR regulation of autophagy. FEBS Lett 584: 1287–1295.

Kim J, Kundu M, Viollet B, Guan K-L (2011). AMPK and mTOR regulate autophagy through direct phosphorylation of Ulk1. Nat Cell Biol 13: 132–141.

King TD, Song L, Jope RS (2006). AMP-activated protein kinase (AMPK) activating agents cause dephosphorylation of Akt and glycogen synthase kinase-3. Biochem Pharmacol 71: 1637–1647.

Li J, Qin Z, Liang Z (2009). The prosurvival role of autophagy in resveratrol-induced cytotoxicity in human U251 glioma cells. BMC Cancer 9: 215.

Pawson AJ, Sharman JL, Benson HE, Faccenda E, Alexander SP, Buneman OP, Davenport AP, McGrath JC, Peters JA, Southan C, Spedding M, Yu W, Harmar AJ; NC-IUPHAR. (2014). The IUPHAR/BPS Guide to PHARMACOLOGY: an expert-driven knowledge base of drug targets and their ligands. Nucl. Acids Res. 42 (Database Issue): D1098–1106.

Sheng Y, Sun B, Guo WT, Zhang YH, Liu X, Xing Y *et al*. (2013). 3-Methyladenine induces cell death and its interaction with chemotherapeutic drugs is independent of autophagy. Biochem Biophys Res Commun 432: 5–9.

Shigemitsu K, Tsujishita Y, Hara K, Nanahoshi M, Avruch J, Yonezawa K (1999). Regulation of translational effectors by amino acid and mammalian target of rapamycin signaling pathways. Possible involvement of autophagy in cultured hepatoma cells. J Biol Chem 274: 1058–1065.

Sun B, Huo R, Sheng Y, Li Y, Xie X, Chen C *et al*. (2013). Bone Morphogenetic protein-4 mediates cardiac hypertrophy, apoptosis, and fibrosis in experimentally pathological cardiac hypertrophy novelty and significance. Hypertension 61: 352–360.

Vucicevic L, Misirkic M, Kristina J, Vilimanovich U, Sudar E, Isenovic E *et al*. (2011). Compound C induces protective autophagy in cancer cells through AMPK inhibition-independent blockade of Akt/mTOR pathway. Autophagy 7: 40–50.

Wang J, Whiteman MW, Lian H, Wang G, Singh A, Huang D *et al*. (2009). A non-canonical MEK/ERK signaling pathway regulates autophagy via regulating Beclin 1. J Biol Chem 284: 21412–21424.

Wong AS, Lee RH, Cheung AY, Yeung PK, Chung SK, Cheung ZH *et al*. (2011). Cdk5-mediated phosphorylation of endophilin B1 is required for induced autophagy in models of Parkinson's disease. Nat Cell Biol 13: 568–579.

Yang YP, Hu LF, Zheng HF, Mao CJ, Hu WD, Xiong KP *et al*. (2013). Application and interpretation of current autophagy inhibitors and activators. Acta Pharmacol Sin 34: 625–635.

Yang Z, Klionsky DJ (2010). Mammalian autophagy: core molecular machinery and signaling regulation. Curr Opin Cell Biol 22: 124–131.

Zhu H, Tannous P, Johnstone JL, Kong Y, Shelton JM, Richardson JA *et al*. (2007). Cardiac autophagy is a maladaptive response to hemodynamic stress. J Clin Invest 117: 1782–1793.

Supporting information

Additional Supporting Information may be found in the online version of this article at the publisher's web-site:

http://dx.doi.org/10.1111/bph.12821

Figure S1 Chemical structures of DMH1 and compound C. DMH1 is a compound C analogue with structural modifications at the 3- and 6-positions in the pyrazolo[1,5-a]pyrimidine backbone.

Figure S2 DMH1 treatment inhibits starvation-induced autophagy responses in HT29 cells. *$P < 0.05$; **$P < 0.01$ versus ST. $n = 3$ individual experiment. CTL, control; ST, starvation.

Figure S3 DMH1 treatment does not inhibit starvation- and AICAR-induced AMPK activation in Hela cells. **$P < 0.01$ versus control. The concentrations of DMH1 and AICAR were 10 μM and 0.5 mM respectively.

Figure S4 DMH1 treatment inhibits starvation-induced GSK3 activation. (A) DMH1 treatment inhibited starvation-induced GSK3 activation in MCF7 cells. $n = 4$. (B) DMH1 treatment inhibited starvation-induced GSK3 activation in HT29 cells. $n = 6$. **$P < 0.01$ versus CTL; #$P < 0.05$, ##$P < 0.01$ versus ST. CTL, control; ST, starvation.